(Article begins on next page)

A 0.2 W Heterostructure Barrier Varactor Frequency Tripler at 113 GHz

Josip Vukusic, Tomas Bryllert, T. Arezoo Emadi, Mahdad Sadeghi and Jan Stake

***Abstract*— We present a high power InAlAs/InGaAs/InP heterostructure barrier varactor (HBV) frequency tripler. The HBV device topology was designed for efficient thermal dissipation and high efficiency. To verify simulations the device was flip-chip soldered onto embedding microstrip circuitry on an aluminum nitride (AlN) substrate. This hybrid circuit was then mounted in a waveguide block without any movable tuners. From the resulting RF-measurements the maximum output power was 195 mW at 113 GHz with a conversion efficiency of 15 %. The measured 3-dB bandwidth was 1.5 %.**

***Index Terms*— heterostructure barrier varactor, frequency multiplier, high-power operation, thermal management, semiconductor diodes, millimeter wave devices, terahertz source**

I. Introduction

Many of the available sources at the frequencies 0.1-3 THz are today bulky, expensive, inefficient and in some cases only operate at cryogenic temperatures. Sources at these frequencies could be exploited in areas such as radio-astronomy, medicine, biology and security imaging. An approach to remedy the lack of efficient sources and allow for a number of applications to flourish is to multiply the output frequency from a fundamental source such as an IMPATT diode, Gunn diode and oscillator circuit [1]. A varactor type of device like the Schottky diode [2] or the Heterostructure Barrier Varactor (HBV) diode is a nonlinear element that can generate higher order frequencies by multiplication. The HBV has the benefit of operating without DC-bias only producing odd multiples of the input frequency i.e 3x,5x,7x,.. . This type of diode is realized by epitaxially growing a heterostructure sequence of low-high-low bandgap material. When a voltage is applied across such a semiconductor material the high bandgap material acts as a barrier for the carriers causing accumulation and depletion of carriers in the respective low bandgap layers. This has the effect of changing the capacitance as a function of the applied voltage C=C(V). It is this nonlinear effect that is utilized for the multiplication of the input frequency. Since the layer sequence can be repeated during growth, several barriers can be stacked to make the device withstand a large voltage amplitude and thus high power. Earlier reports of high output power from an HBV demonstrated 91 mW at 93 GHz with a conversion efficiency of 10 % [3]. Experimental results at higher frequencies have been reported producing 9.5 mW at 300 GHz with a conversion efficiency of 8 % [4] and 6 mW at 288 GHz [5] with an integrated circuit approach. State-of-the-art results for multipliers based on Schottky diodes are exemplified by a doubler producing 300 mW at 99 GHz [6].

In this report we present state-of-the-art results from an HBV based tripler designed for high output power. The design and fabrication of the HBV device and circuit are described below, followed by an account of the measurement setup and results.

II. Design and Fabrication

Because of the high power pumped into the HBV device, care has to be taken to - alongside the electrical calculations - include and optimize the thermal aspect [7-9] of the tripler operation. The epi-material is a generic HBV design [10] with three barriers in order to operate at high voltages. For this structure the modulation layer is 250 nm with a doping concentration of $1x10^{17}$ cm^{-3} and a 13 nm barrier thickness.

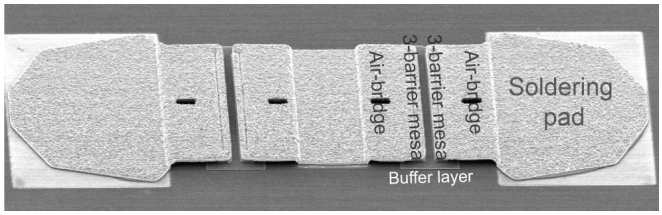

Fig. 1. SEM micrograph of a 500 μm^2 HBV. This 4-mesa, 12-barrier device is processed from Chalmers MBE1038 epitaxial material.

We chose the symmetric, planar topology [11-13] for the HBV device. But instead of the conventional two mesas we have connected four mesas in series as seen from the SEM micrograph in figure 1. The reason for this is twofold; growing 6 barriers in the pseudomorphic AlAs/InAlAs/InGaAs material system is difficult, also the InGaAs alloy has a magnitude lower thermal conductivity than the InP substrate, resulting in poor thermal dispersion when growing a thick epitaxy. Finite-Element-Method (FEM) calculations revealed a reduction of the thermal resistance by a factor of two using the 4-mesa 3-barrier topology. Both the mentioned reasons call for a thin epitaxy and therefore few barriers. So even though the material itself is only 3 barriers 'thick', the total number of barriers for the 4 mesas in series is 3x4=12. To reduce the series resistance through the connecting buffer layer, the four mesas were elongated with an aspect ratio of 14:1. This also increases the thermal cross-section through the gold air-bridges.

The embedding impedances were optimized using Agilent Advanced Design System, in which the Chalmers electro-thermal HBV model [14] has been implemented. This model self-consistently calculates the interdependent electrical and thermal properties of the device. 3-dimensional FEM modeling was applied to calculate the thermal resistance and

Thanks to Carl-Magnus Kihlman for machining the waveguide block. This work has been supported by the Swedish Defense Research Agency (FOI), Swedish Foundation for Strategic Research (SSF) and the European Space Agency (ESA).

The authors are with the Terahertz and Millimetre Wave Laboratory, Department of Microtechnology and Nanoscience, Chalmers University of Technology, SE-412 96 Göteborg, Sweden (e-mail: vukusic@chalmers.se).

electrical series resistance used in the model. Ansoft HFSS 3D electromagnetic solver was used to design the microstrip circuitry and waveguide block. AlN was chosen as substrate for the microstrip circuitry, due to its high thermal conductivity (~ 170 W/mK).

The epitaxial material was grown by molecular beam epitaxy (EPI930) at the Nanofabrication Laboratory at Chalmers. Standard III-V processing techniques were used to fabricate the HBV devices. Photolithography (PL) was employed to pattern the contacts onto image-reversal photoresist. This was then followed by e-beam evaporation of the layer sequence Au/Ge/Ni for n-contact formation. On top of the the n-contacts a layer of silicon nitride (Si3N4) was deposited at room temperature using plasma enhanced chemical vapor deposition to serve as etch mask when defining the mesas. Lift-off in a photoresist solvent was then performed to remove the superfluous Si3N4/Au/Ge/Ni layer surrounding the mesas. After ohmic contact annealing the mesas were dry etched by means of an inductively coupled plasma (ICP) in a CH4/H2/Ar gas mixture. The remnants of the Si3N4 were subsequently removed by ICP dry etching in NF3 gas.

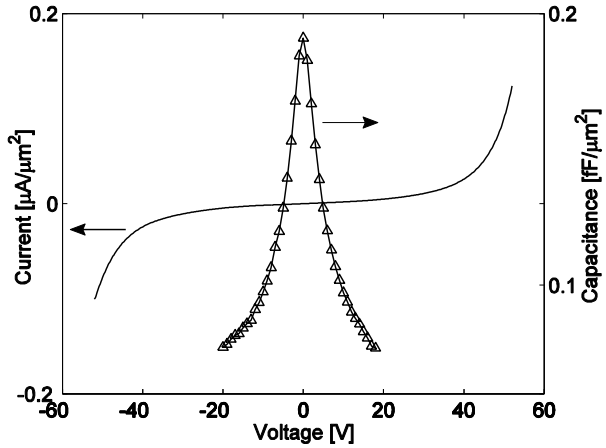

Fig. 2. Graph showing the I-V and C-V curves measured on a 12-barrier, 700 μm^2 HBV. Note the high breakdown voltage of ≥ 50 V.

To isolate the devices a PL pattern masked for the selective wet etchant H3PO4/H2O2/H2O, removing all of the epitaxial layers down to the SI-InP substrate. For the air-bridge formation a layer of photoresist was cleared at the mesa and contact pad sites by PL patterning. The whole chip was then covered by a seed layer of gold, which was deposited by magnetron sputtering. Another photoresist layer was patterned to define the air-bridge fingers and the entire chip was gold electro-plated to a thickness of ~2 μm. Ion beam etching was utilized to sputter away the thin seed layer connecting the plated areas. Figure 1 shows a SEM image of a fabricated 4-mesa, 12-barrier device. The DC-characteristics from such a device is presented in Figure 2. This graph shows the characteristic anti-symmetric I-V and symmetric C-V curves. From this graph we can notice the high breakdown voltage of ≥ 50 V for this 12-barrier HBV. This value of the breakdown voltage is 20 V lower than what is expected when scaling one barrier to twelve. The reason for this discrepancy could be processing imperfections and/or issues related to measuring with our DC characterization equipment at high voltages.

The circuit was defined using PL and subsequently gold plated to define the microstrip elements. Both the HBV device on the InP substrate and microstrip circuit on the AlN substrate were lapped down to a thickness of 40/100 μm respectively. The devices/circuits were then diced and the HBVs flip-chip soldered onto the microstrip. This hybrid circuit was then mounted in the waveguide block with a WR22/WR10 input and output respectively. The two-piece, waveguide block with dimensions 30x30x42 mm3 was fabricated from brass and gold electro-plated. Figure 3 shows a photograph of the AlN microstrip circuit mounted in one half of the waveguide block. This image features a description of the different circuit elements included on the substrate such as waveguide probes and a low-pass filter. The waveguide block has no movable tuners.

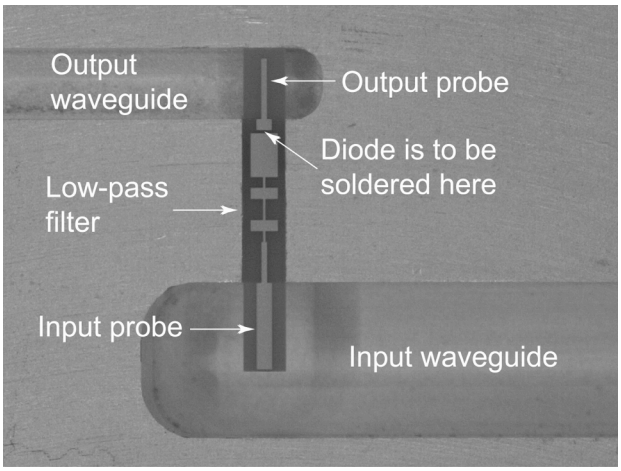

Fig. 3. Photograph depicting an AlN microstrip circuit mounted in the waveguide block.

III. Results and Discussion

The measurement setup consists of a HP83650B signal generator, a SpaceK Labs power amplifier SP342-35-31, an isolator, waveguide block and Ericson PM2 power meter. These instruments were connected in series in the order mentioned. At the output of the isolator, before the multiplier input, the available input power was measured with a calibrated 20 dB attenuator and an Agilent E4419B power meter. To verify the matching at the input we also used a 10 dB directional coupler between the input of the waveguide block and the isolator. The reflected power at the directional coupler was measured by means of the Agilent E4419B power meter. Figure 4 shows the measured output power as a function of the input power, and we can see that the maximum output power is 195 mW at 113 GHz. Plotted in this graph is also the conversion efficiency with a maximum of 15 % for high input powers. The drastic increase of efficiency above 0.4 W is accredited to a voltage-swing dependent impedance and Cmax/Cmin ratio. The maximum input power was 1.3 W. We also measured a fixed-power frequency sweep presented in Figure 5. The 3-dB bandwidth which is centered around

113.25 GHz was found to be ~ 1.5 %. This is mainly attributed to the bandwidth of the embedding circuitry, i.e. the passive circuit on the AlN substrate. Measurements with the directional coupler connected showed that for high input powers the reflected power was less than 7 % which indicates good matching at the input.

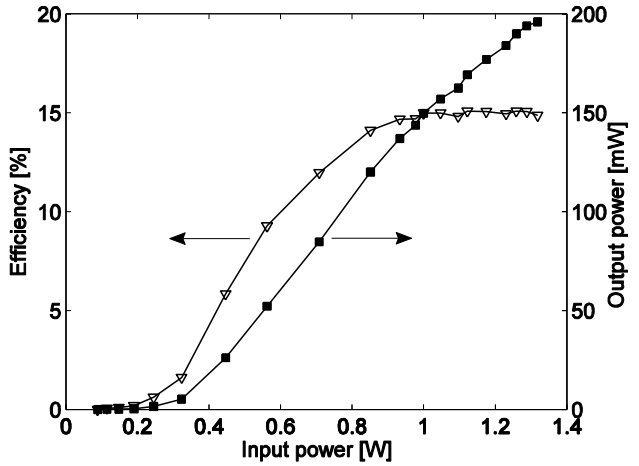

Fig. 4. Graph showing the output power and efficiency from a 700 μm^2, 12-barrier HBV tripler.

During the design process the circuit was tuned to a center frequency 104 GHz. The deviation from target frequency for the measured results is believed to stem from uncertainties in the AlN material parameters and device fabrication. Further modeling has shown that by tuning the material parameters used in the calculations and improving the microstrip circuit design significant improvements in output power, conversion efficiency and 3-dB bandwidth is to be expected. Experimental reports have shown that a conversion efficiency of over 20 % is feasible for frequencies around 100 GHz [15].

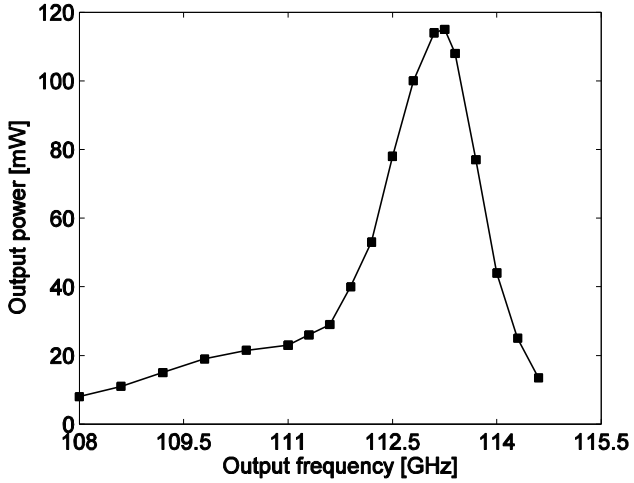

Fig. 5. Graph showing the output power from the HBV tripler for a fixed input power of 0.8 W at different output frequencies.

IV. Conclusions

We have designed, fabricated and characterized an HBV based frequency tripler intended for high output power. The devices were fabricated from AlAs/InAlAs/InGaAs/InP epitaxial material, while the microstrip circuit was realized on an AlN carrier substrate. The high frequency measurements showed state-of-the-art results, increasing the output power at ~100 GHz by a factor of two compared to previous reports on HBV based multipliers. The maximum output power was 195 mW at 113 GHz with a conversion efficiency of 15 %. Additional simulations of an augmented circuit design show performance improvements and is expected to yield further increases in output power, efficiency and 3-dB bandwidth

References

[1] "Two-terminal active devices for terahertz sources", Haddad, G.I.; East, J.R.; Eisele, H. Source: International Journal of High Speed Electronics and Systems, v 13, n 2, June 2003, p 395-427

[2] "Capability of THz sources based on Schottky diode frequency multiplier chains", Ward, J.; Schlecht, E.; Chattopadhyay, G.; Maestrini, A.; Gill, J.; Maiwald, F.; Javadi, H.; Mehdi, I.; Microwave Symposium Digest, 2004 IEEE MTT-S International Volume 3, 6-11 June 2004 Page(s):1587-1590 Vol.3

[3] "A W-band medium power multi-stack quantum barrier varactor frequency tripler", Rahal, A.; Bosisio, R.G.; Rogers, C.; Ovey, J.; Sawan, M.; Missous, M.; Microwave and Guided Wave Letters, IEEE, Vol. 5, Issue 11, Nov. 1995 Page(s):368-370

[4] "High-efficiency heterostructure-barrier-varactor frequency triplers AlN substrates", Qun Xiao; Hesler, J.L.; Crowe, T.W.; Weikle, R.M., II; Yiwei Duan; Deaver, B.S.; Microwave Symposium Digest, 2005 IEEE MTT-S International 12-17 June 2005 Page(s):4 pp. 443-446.

[5] "Monolithic integrated circuits incorporating InP-based heterostructure barrier varactors", David, T.; Arscott, S.; Munier, J.-M.; Decoopman, T.; Beaudin, G.; Lippens, D.; IEEE Microwave and Wireless Components Letters, Vol. 12, n. 8, August 2002, pp. 281-283,

[6] D. Porterfield, J. Hesler, T. Crowe, W. Bishop, and D. Woolard, "Integrated terahertz transmit/receive modules," in Proc. 33rd Eur. Microw. Conf., Oct. 7–9, 2003, vol. 3, pp. 1319–1322.

[7] "Thermal constraints for heterostructure barrier varactors", Ingvarson, M.; Alderman, B.; Olsen, Ai.; Vukusic, J.; Stake, J.; Electron Device Letters, IEEE Volume 25, Issue 11, Nov. 2004 Page(s):713-715

[8] "Heterostructure-barrier-varactor design", Stake, J.; Jones, S.H.; Dillner, L.; Hollung, S.; Kollberg, E.L.; Microwave Theory and Techniques, IEEE Transactions on Volume 48, Issue 4, Part 2, April 2000 Page(s):677-682

[9] "Effects of self-heating on planar heterostructure barrier varactor diodes", Stake, J.; Dillner, L.; Jones, S.H.; Mann, C.; Thornton, J.; Jones, J.R.; Bishop, W.L.; Kollberg, E.; Electron Devices, IEEE Transactions on Volume 45, Issue 11, Nov. 1998 Page(s):2298–2303

[10] "Heterostructure barrier varactors on copper substrate", Dillner, L.; Stake, J.; Kollberg, E.L.;Electronics Letters Volume 35, Issue 4, 18 Feb. 1999 Page(s):339-341

[11] "Planar multibarrier 80/240-GHz heterostructure barrier varactor triplers", Jones, J.R.; Bishop, W.L.; Jones, S.H.; Tait, G.B.; Microwave Theory and Techniques, IEEE Transactions on Volume 45, Issue 4, April 1997 Page(s):512–518

[12] "11% efficiency 100 GHz InP-based heterostructure barrier varactor quintupler", Bryllert, T.; Olsen, A.; Vukusic, J.; Emadi, T.A.; Ingvarson, M.; Stake, J.; Lippens, D.;Electronics Letters Volume 41, Issue 3, 3 Feb 2005 Page(s):131–132

[13] "Fabrication and performance of InP-based heterostructure barrier varactors in a 250-GHz waveguide tripler", Melique, X.; Maestrini, A.; Farre, R.; Mounaix, P.; Favreau, M.; Vanbesien, O.; Goutoule, J.-M.; Mollot, F.; Beaudin, G.; Narhi, T.; Lippens, D.;Microwave Theory and Techniques, IEEE Transactions on, Volume 48, Issue 6, June 2000 Page(s):1000-1006

[14] "An electro-thermal HBV model", Ingvarson, M.; Vukusic, J.; Oistein Olsen, A.; Arezoo Emadi T; Stake, J.; Microwave Symposium Digest, 2005 IEEE MTT-S International 12-17 June 2005 Page(s):1151-1153

[15] "HBV tripler with 21% efficiency at 102 GHz", Vukusic, J.; Alderman, B.; Emadi, T.A.; Sadeghi, M.; Olsen, A.O.; Bryllert, T.; Stake, J.; Electronics Letters Volume 42, Issue 6, 16 March 2006 Page(s):355-356